Simple theory of atom-surface scattering

Tsofar Maniv
Department of Chemistry and the Solid State Institute, Technion-Israel Institute of Technology, Haifa 32000, Israel and Exxon Research and Engineering Company, Corporate Research Science Laboratories, Clinton Township, Route 22 East, Annandale, New Jersey 08801

Morrel H. Cohen
Exxon Research and Engineering Company, Corporate Research Science Laboratories, Clinton Township, Route 22 East, Annandale, New Jersey 08801

(Received 11 February 1985)

The theory of the scattering of a beam of particles by a corrugated surface potential is shown to simplify dramatically in the semiclassical limit if the corrugation is not too strong and the direction of the incoming beam is close to the surface normal. It is shown that in any scattering event by a potential of quite general form the scattering amplitude is dominated by the potential corrugation near vanishing potential. For a weakly corrugated Morse potential, it is found that under near-normal-incidence conditions the classical scattering cross section is identical to the corresponding cross section for scattering by a hard corrugated wall with the same corrugation. Quantum-mechanical effects appear as small oscillations about the Kirchoff scattering amplitude. It is proposed that the observation of pronounced neon diffraction from Ni(110) and Pd(110), reported recently, may be reasonably explained if the corrugation function is defined at vanishing potential rather than at the classical turning points.

I. INTRODUCTION

Recently, there has been significant progress in developing powerful numerical techniques for calculating cross sections for scattering of atomic and molecular beams from solid surfaces.[1–10] This progress in the scattering theory has already led to improved understanding of the nature of the gas-surface interaction in the relevant range of potential energies.[2–6]

In particular, a sensitivity test made by Perreau and Lapujoulade,[2] using a method developed by Armand and Manson,[3–5] has shown that the scattering cross sections obtained by using realistic model potentials can deviate considerably from those obtained by using the highly popular hard-corrugated-wall (HCW) model.[11,12] Furthermore, a comparison between the results obtained for a soft potential which includes an attractive well[5] (a corrugated Morse potential) and the results obtained for a purely repulsive, soft potential[3,4] (a corrugated exponential potential) has shown remarkable disagreement[2] even for incident beam energies much larger than the potential well depth.

The great sensitivity of the gas-surface scattering processes to the details of the atom-surface interaction potential, implied by these theoretical analyses, is unfortunate in that it implies that the structural information that one hopes to extract from atom diffraction data[13–15] should be obtained through large-scale numerical computations with only little physical insight at the end of the computational process. The lack of physical insight is a far more serious problem in cases where inelastic effects,[16–19] which involve excitations of the solid degrees of freedom, are of significant importance, since in most cases of interest (except for very low incident energies[20,21]) only very drastic approximations can avoid untractable computations.

In a recent paper[22] we have shown, however, that a search for a simple theoretical picture is not completely hopeless; we have discovered that in the classical limit the scattering amplitude from any potential is dominated by the potential corrugation near vanishing potential (i.e., near the crossover of the potential from attraction to repulsion). Under certain conditions (i.e., for incoming beams very close to normal incidence and for surfaces which are not too corrugated), the sensitivity of the scattering process to the details of the potential is found to be reduced considerably so that the scattering amplitudes obtained for a soft potential are very close to those obtained for an infinitely hard corrugated potential.

In this paper we present the theory which yields the analytic results reported in Ref. 22 and discuss in greater detail the validity and implications of these results. We also present here some numerical results which greatly facilitate the above-mentioned discussions.

The organization of the paper is as follows: In Sec. II we present the general semiclassical formulation used in this paper and some important results of a general nature (e.g., the vanishing potential theorem). In Sec. III we specialize our discussion to a model potential and describe an iterative procedure for solving the corresponding Hamilton-Jacobi equation for the phase of the scattering wave functions. In Sec. IV we derive a simple Kirchoff-like expression for the scattering T matrix, which is valid for incident beams close to normal incidence and for weakly corrugated potentials. In Sec. V we present our numerical results and discuss their implications.

II. THE SCATTERING AMPLITUDE IN THE SEMICLASSICAL LIMIT

We consider the scattering of a monochromatic beam of atoms by a corrugated surface potential $V(\mathbf{R},z)$, where $\mathbf{R}$ stands for the projection of the position vector $\mathbf{r}$ onto the nominal surface plane. The scattering wave functions are normalized in a three-dimensional rectangular box of macroscopic sides L_x, L_y, and L_z, where the nominal surface plane at $z=0$ cuts the box into two equal regions. The free-particle region corresponds to negative values of z.

The on-shell (elastic) scattering probability amplitude, $f(\mathbf{p},\mathbf{p}')$, from the initial asymptotic momentum $\mathbf{p}\equiv(\mathbf{P},p_z)$, $p_z>0$, to the final asymptotic momentum $\mathbf{p}'\equiv(\mathbf{P}',p_z')$, $p_z'\le 0$, is given by

$$f(\mathbf{p},\mathbf{p}')=-\delta_{p,p'}e^{-(i/\hbar)\epsilon_p t_0}T_E(\mathbf{p},\mathbf{p}')\ , \tag{1}$$

where $p\equiv|\mathbf{p}|$, $\epsilon_p\equiv\hbar^2p^2/2M_G$, M_G is the mass of the atom, t_0 is the time of a round trip for the atom from and to the box edge plane $z=-L_z/2$, and $T_E(\mathbf{p},\mathbf{p}')$ is the on-shell T matrix:[23]

$$T_E(\mathbf{p},\mathbf{p}')\equiv(t_0/\hbar)\int d^3r_1\int d^3r_2 e^{(i/\hbar)\mathbf{p}\cdot\mathbf{r}_1}\times V(\mathbf{r}_1)G_E(\mathbf{r}_1,\mathbf{r}_2)\times V(\mathbf{r}_2)e^{-(i/\hbar)\mathbf{p}'\cdot\mathbf{r}_2}\ . \tag{2}$$

$G_E(\mathbf{r}_1,\mathbf{r}_2)$ is the propagator for the atom from $\mathbf{r}_1$ to $\mathbf{r}_2$ at energy E. The value of t_0 can be readily obtained in terms of L_z, p_z, and p_z', i.e.,

$$t_0=L_zM_G\overline{|p_z|}/|p_zp_z'|\ , \tag{3}$$

where

$$\overline{|p_z|}\equiv\tfrac{1}{2}(|p_z|+|p_z'|)\ .$$

To calculate G_E we shall use the spectral expansion

$$G_E(\mathbf{r}_1,\mathbf{r}_2)=\sum_n\psi_n^*(\mathbf{r}_1)\psi_n(\mathbf{r}_2)/(E_n-E)\ , \tag{4}$$

where $\{\psi_n(\mathbf{r})\}$ is a complete orthogonal set of eigenstates with energies E_n. A semiclassical wave function can be written in the form

$$\psi_{\mathbf{K},q_z}(\mathbf{r})=(L_xL_yL_z)^{-1/2}[A^{\text{inc}}_{\mathbf{K},q_z}(\mathbf{r})e^{(i/\hbar)S^{\text{inc}}_{\mathbf{K},q_z}(\mathbf{r})}+A^{\text{ref}}_{\mathbf{K},q_z}(\mathbf{r})e^{(i/\hbar)S^{\text{ref}}_{\mathbf{K},q_z}(\mathbf{r})}]\ , \tag{5}$$

where

$$E_{\mathbf{K},q_z}\equiv\frac{\hbar^2}{2M_G}(K^2+q_z^2)\ , \tag{6}$$

and $\hbar\mathbf{K}$ is the asymptotic momentum parallel to the nominal surface plane. The action $S_{\mathbf{K},q_z}(\mathbf{r})$, with either of the superscripts inc or ref, corresponding to either the incident or to the reflected wave, respectively, is the solution of the Hamilton-Jacobi equation,[24]

$$\left[\frac{\partial S_{\mathbf{K},q_z}}{\partial\mathbf{r}}\right]^2=2M_G[E_{\mathbf{K},q_z}-V(\mathbf{r})]\ , \tag{7}$$

while the amplitude $A_{\mathbf{K},q_z}$ is given by[25]

$$A^2_{\mathbf{K},q_z}(\mathbf{r})\equiv\det\left[\frac{\partial^2S_{\mathbf{K},q_z}(\mathbf{r})}{\partial x_i\,\partial k_j}\right]\Big/\hbar\ ,\qquad x_i\equiv(\mathbf{R},z),\ \ k_j\equiv(\mathbf{K},q_z)\ . \tag{8}$$

Using Eq. (5) in Eq. (4) and then substituting Eq. (4) into Eq. (2), we obtain, after integrating over q_z,

$$T(\mathbf{p},\mathbf{p}')=\overline{|p_z|}(4\pi^2\Omega)^{-1}\int d^2K\,f(\mathbf{p};\mathbf{K})f^*(\mathbf{p}';\mathbf{K})/\hbar k_z\ , \tag{9}$$

where

$$f(\mathbf{p};\mathbf{K})\equiv(M_G/i\hbar p_z)\times\int d^3r\,V(\mathbf{r})A^{\text{inc}}_{\mathbf{K},k_z}(\mathbf{r})\times\exp\{(i/\hbar)[\mathbf{p}\cdot\mathbf{r}-S^{\text{inc}}_{\mathbf{K},k_z}(\mathbf{r})]\}\ , \tag{10}$$

$$\hbar k_z\equiv(2M_GE-\hbar^2K^2)^{1/2}\ ,$$

Ω is the illuminated surface area ($=L_xL_y$), and $f^*(\mathbf{p}_z';\mathbf{K})$ is obtained by replacing p_z, A^{inc}, and S^{inc} in Eq. (10) by p_z', A^{ref}, and S^{ref}, respectively. Note that in Eq. (10) $f(\mathbf{p};\mathbf{K})$ is exclusively determined by the quantities characterizing the incident wave. In general, however, the reflected wave should also contribute to $f(\mathbf{p};\mathbf{K})$, but this contribution is negligible under the semiclassical conditions considered here (see below). Similarly, there is no contribution to $f^*(\mathbf{p}';\mathbf{K})$ from the incident wave within the semiclassical approximation used here.

Let us now apply the stationary-phase (SP) method to the three-dimensional integral in Eq. (10). This approximation is, of course, consistent with the semiclassical limit. The corresponding stationary point $\mathbf{r}_0$ satisfies the equation

$$\left[\frac{\partial S^{\text{inc}}_{\mathbf{K}}}{\partial\mathbf{r}}\right]_{\mathbf{r}_0}=\mathbf{p}\ , \tag{11}$$

so that, together with the Hamilton-Jacobi (HJ) equation [Eq. (7)],

$$\left[\frac{\partial S^{\text{inc}}_{\mathbf{K}}}{\partial\mathbf{r}}\right]^2=2M_G[E-V(\mathbf{r})]=p^2-2M_GV(\mathbf{r})\ , \tag{12}$$

one finds that $\mathbf{r}_0$ should lie on the equipotential surface $V(\mathbf{r})=0$.[22] The argument for $f(\mathbf{p}';\mathbf{K})$ is similar: The stationary point $\mathbf{r}_0'$ satisfies the equation

$$\left[\frac{\partial^{\text{ref}}_{\mathbf{K}}}{\partial\mathbf{r}}\right]_{\mathbf{r}_0'}=\mathbf{p}'\ , \tag{11'}$$

and the HJ equation reads

$$\left[\frac{\partial S^{\text{ref}}_{\mathbf{K}}}{\partial\mathbf{r}}\right]^2=p'^2-2M_GV(\mathbf{r})\ , \tag{12'}$$

so that $\mathbf{r}_0'$ also lies on the surface $V(\mathbf{r})=0$.

Note that the basic integrand [Eq. (10)] vanishes at the point of SP so that the leading contribution to the integral from this point is zero. It is, therefore, required to carry out an unconventional SP integration, in which the preexponential is expanded to higher orders about the point of SP. As we shall show later in this paper, already the first-order approximation yields the well-known exact result for the classical limit reflection coefficient in one-dimensional systems.

Up to this point our analysis has been quite general, provided the semiclassical limit is assumed. To proceed along these general lines would be, however, a formidable task. It would be therefore instructive to consider the scattering in a one-dimensional (1D) system, for which one may still keep the form of the potential $V(z)$ quite general when the SP integration is carried out. The result of such a procedure should be universal [i.e., independent of the specific form of $V(z)$] since the scattering probability (reflection coefficient) in one dimension equals unity below the barrier in the semiclassical limit. In a 1D system $f(p_z;0)$ (which is just the reflection amplitude) is given by

$$f(p_z;0)=(M_G/i\hbar p_z)\int_{-\infty}^{\infty} dz\, V(z)A^{\rm inc}(z) \times e^{(i/\hbar)[p_z z - S^{\rm inc}(z)]}\ , \tag{13}$$

where

$$A^{\rm inc}(z)=\{p_z/[p_z^2-2M_G V(z)]^{1/2}\}^{1/2}\ . \tag{14}$$

Transforming the integral over the spatial variable z to an integral over the potential, i.e., defining a new variable of integration $u\equiv V(z)/D$, where D is the potential-well depth, and then expanding the phase

$$(1/\hbar)[p_z z(u)-S^{\rm inc}(u)]$$

to second order and the amplitude $A^{\rm inc}(u)$ to zeroth order about the stationary point $u=0$, we have

$$f(p_z;0)=(M_G D/i\hbar p_z)\left[\int_0^{-1} u\left[\frac{dz_-}{du}\right]e^{i\lambda u^2}du+\int_{-1}^{\infty}u\left[\frac{dz_+}{du}\right]e^{i\lambda u^2}du\right]\exp\left[\frac{i}{\hbar}[p_z z_+(0)-S^{\rm inc}(0)]\right]\ , \tag{15}$$

where

$$\lambda=(M_G D/2p_z\hbar\chi)\ ,$$

and (16)

$$\chi\equiv\left[\frac{du}{dz}\right]_{u=0}\ .$$

The functions $z_{+,-}(u)$, appearing in Eq. (15), are the two solutions of the equation $V(z)=Du$ in the range $-1\le u\le 0$ (i.e., within the attractive well), $z_+(u)$ being the solution for which $dz/du>0$, while $z_-(u)$ is the solution with $dz/du<0$ (we assume that the potential has only a single minimum). Note that the stationary-phase equation, $u=0$, has also two solutions, $z_-(0)=-\infty$ and $z_+(0)$, which are located at the crossover point between the attractive and the repulsive regions of the potential. At the former point, however, the phase

$$\frac{1}{\hbar}[p_z z(u)-S^{\rm inc}(u)]$$

has an essential singularity since all the derivatives of u with respect to z vanish there. Thus the only stationary point around which an analytic expansion exists is the latter one.

Equation (15) shows that if the value of the parameter λ [Eq. (16)] is of the order of unity or larger, the integrals in Eq. (15) are very sensitive to the detailed shape of the potential well as reflected by the values of $dz_{+,-}/du$ in the region $-1\le u\le 0$. This seems rather surprising since one usually expects that the effect of the attractive potential well on the scattering process would be important only if the values of the parameter $\gamma\equiv D/E_{iz}$ (E_{iz} being the energy of the incident beam) become of the order unity or larger. In the semiclassical limit, however, $\lambda=\gamma(p_z/4\hbar\chi)\gg\gamma$, so that large values of λ do not necessarily mean large values for γ. If E_{iz} is sufficiently large, however, such that $\lambda\ll 1$, the important region of integration in Eq. (15) (i.e., $u\le 1/\sqrt{\lambda}$) is considerably larger than the potential-well region, and the detailed behavior of $dz_{+,-}/du$ in the region $-1<u<0$ should not affect the value of the integral in any significant way. Under these circumstances we may replace both dz_+/du and dz_-/du in Eq. (15) by the value of dz_+/du at the stationary point $z_+(0)$ (i.e., by χ^{-1}), so that

$$f(p_z;0)=-[\exp(i\phi)]2i\lambda\int_0^{\infty}u\,e^{i\lambda u^2}du\ , \tag{17}$$

where

$$\phi\equiv\frac{1}{\hbar}[p_z z_+(0)-S^{\rm inc}(0)]\ .$$

The integral appearing in Eq. (17) is ill behaved at the upper limit of the integration due to the breakdown of the expansion about $u=0$ for large values of u. Nevertheless, by introducing a small, positive imaginary part into λ to destroy the artificial oscillations at large u, the trivial integration in Eq. (17) yields the result

$$|f(p_z;0)|^2=|e^{i\phi}|^2=1\ , \tag{18}$$

which is identical to the exact result for the reflection coefficient below the barrier in 1D systems.

The accuracy of the simple SP procedure described above can be further and more significantly tested by applying it to an analytically soluble problem such as a particle in a 1D Morse potential and comparing the result with an exact numerical integration. As we shall see later (see Sec. IV A), the two methods are in excellent agreement provided that $\lambda\ll 1$.

The major surprise of this result is the negligible role played by the classical turning point. In fact, the exact integrand [see Eq. (13)] diverges at the classical turning point, due to the breakdown of the semiclassical approximation there. In our approximate expression [Eq. (15)]

we have replaced the term responsible for the singularity [i.e., the amplitude $A^{\rm inc}(z)$, Eq. (14)] by its value at the stationary point $u=0$. This replacement is a terrible approximation near the classical turning point. It turns out, however, that in both the exact integral and the approximate one the contribution coming from the region around the classical turning point is completely washed out by the oscillations of the integrand there. This important point is illustrated in Fig. 1, where the exact integrand in Eq. (13) for a 1D Morse potential (for which the solution of the HJ equation is known analytically) is plotted together with a modified version of the same integrand, in which the amplitude $A^{\rm inc}(z)$ is replaced by the value of $A^{\rm inc}(z)$ at the stationary point. It is clearly seen that both the exact and the approximate integrands oscillate symmetrically about zero near the classical turning point so that despite the large difference between them in this region the overall integrals are almost identical.

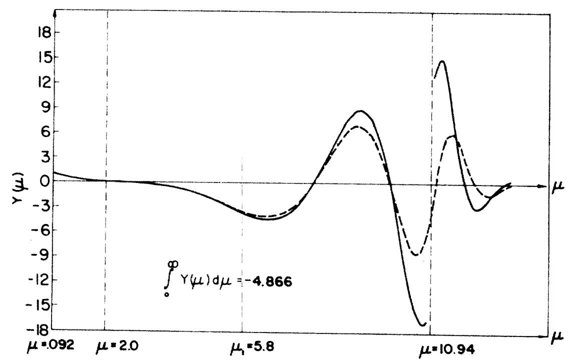

FIG. 1. The solid line represents the imaginary part $Y(\mu)$ of the integrand in Eq. (41) for $k_{z,0}=(1/\hbar)p_z$, $\nabla\zeta=0$ ($U=1$), corresponding to reflection by a one-dimensional (1D) Morse potential [see Eq. (19) with $\zeta=0$], as a function of $\mu=e^{\chi z}$. The dashed line represents the same function except that $W(\mu)$ is replaced by unity. The parameters used are $k_{z,0}/\chi=34.36$, $\gamma\equiv D/E_{iz}=0.0102$. The classical turning point corresponds to $\mu=10.94$. The corresponding reflection coefficients obtained by integrating numerically Eq. (41) are $|B|^2=0.9975$ for the exact integrand and $|B|^2=0.957$ for the integrand with $W(\mu)=1$. Note that $\int_0^{\mu_1} Y(\mu)d\mu \approx \int_0^{\infty} Y(\mu)d\mu=-4.866$, where $\mu_1=5.8$.

III. SOLVING THE HJ EQUATION FOR A WEAKLY CORRUGATED MORSE POTENTIAL

The general analysis of Sec. II implies that for realistic potentials (i.e., soft potentials which include both attractive and repulsive parts) the scattering amplitudes $f(\mathbf{p};\mathbf{K}), f^*(\mathbf{p}',\mathbf{K})$ gain most of their contributions in a restricted region of space, near the crossover of the potential from attraction to repulsion, far away from the classical turning point. In other words, due to mismatch between the free-particle incident wave and the fully distorted incident wave in regions where the potential is strong, there is gross cancellation of scattering amplitude generated in these regions, leaving a restricted region around the vanishing potential as important to the scattering process.

To calculate the scattering T matrix in Eq. (9) it is, therefore, not necessary to solve the HJ equation in the entire space but only to find an expansion for the action $S^{\rm inc}_{\mathbf{K},k_z}$, which converges rapidly within the important region around the vanishing potential. Fortunately this region is located far away from the classical turning point, where the use of the semiclassical approximation is quite safe.

Our aim in this section is, therefore, to find an approximate analytic solution to the HJ equation [Eq. (12)] in the surface region around $V=0$ for a realistic model potential. We select a corrugated Morse (CM) potential of the form

$$V(\mathbf{R},z)=D\mu^2-2D\mu,\quad \mu(\mathbf{R},z)\equiv e^{\chi[z-\zeta(\mathbf{R})]}\,, \tag{19}$$

where $\zeta(\mathbf{R})$ is the corrugation function of the potential, χ is the softness parameter, and D is the potential-well depth. We prefer to use this potential rather than the more popular CM potential,[1,5,26,27] which is assumed to be corrugated only in the repulsive part, because of its relative simplicity and because the latter potential neglects the corrugation of the attractive part. This neglect yields, of course, more realistic behavior in the far-field region but introduces unrealistic behavior in the most important region, namely near the vanishing potential, where both the attractive and the repulsive parts of any model potential used should have the same corrugation to mimic correctly the behavior of the actual potential there (see below).

We assume that the corrugation is weak, i.e., that

$$|\nabla\zeta(\mathbf{R})|^2 \ll 1,\quad \nabla\equiv\frac{\partial}{\partial\mathbf{R}} \tag{20}$$

and that the semiclassical approximation holds, i.e.,

$$k_0\equiv(2M_G E_i/\hbar^2)^{1/2} \gg \chi\,.$$

We shall then solve Eq. (12) iteratively in the small parameter $|\nabla\zeta|$. To do so we shall transform the coordinates $(\mathbf{R},z)$ in Eq. (12) to a new set of coordinates $(\mathbf{R},\mu)$. The new HJ equation then reads

$$(\chi\mu)^2[1+(\nabla\zeta)^2]\left[\frac{\partial S_{\mathbf{K}}}{\partial\mu}\right]^2+\left[\frac{\partial S_{\mathbf{K}}}{\partial\mathbf{R}}\right]^2-2(\chi\mu)\left[\frac{\partial S_{\mathbf{K}}}{\partial\mu}\right]\left[\frac{\partial S_{\mathbf{K}}}{\partial\mathbf{R}}\right]\cdot\nabla\zeta=2M_G[E_i-V(\mu)]\,, \tag{21}$$

where we use the shortened notation $S_{\mathbf{K}}$ for $S_{\mathbf{K},k_z}$. Equation (21) will now be solved iteratively in the small quantities $\nabla\zeta$. To zeroth order we get

$$(\chi\mu)^2\left[\frac{\partial S_{\mathbf{K}}^{(0)}}{\partial\mu}\right]^2+\left[\frac{\partial S_{\mathbf{K}}^{(0)}}{\partial\mathbf{R}}\right]^2=2M_G[E_i-V(\mu)]\ , \tag{22}$$

which is separable in $\mathbf{R}$ and μ and can be readily integrated to yield

$$S_{\mathbf{K}}^{(0)}(\mathbf{R},\mu)=\hbar\mathbf{K}\cdot\mathbf{R}\pm\widetilde{S}(\mu)\ , \tag{23}$$

where

$$\widetilde{S}(\mu)\equiv\frac{1}{\chi}\int\frac{d\mu}{\mu}[\hbar^2k_z^2-2M_GV(\mu)]^{1/2}=(\hbar k_z/\chi)\left[W(\mu)-\sqrt{\gamma}\sin^{-1}\left[\frac{\sqrt{\gamma}(1-\mu)}{\sqrt{1+\gamma}}\right]+\ln\{2\mu/[1+\gamma\mu+W(\mu)]\}\right]\ ,$$

$$\gamma\equiv D/(\hbar^2k_z^2/2M_G)\ \text{ and }\ W(\mu)\equiv(1+2\gamma\mu-\gamma\mu^2)^{1/2}\ . \tag{24}$$

Note that the plus sign in (23) corresponds to the incident wave while the minus sign corresponds to the reflected wave. Note also that $\widetilde{S}(\mu)$ is the classical action for a particle with energy $\hbar^2k_z^2/2M_G$ in a one-dimensional Morse potential $V(\mu)=D\mu^2-2D\mu$. In order to get $S_{\mathbf{K}}$ to first order in $\nabla\zeta$, we substitute the zeroth-order expression for $\partial S_{\mathbf{K}}/\partial\mathbf{R}$ (i.e., $\hbar\mathbf{K}$) and neglect $(\nabla\zeta)^2$ in Eq. (21). The resulting equation is thus written as

$$\left[(\chi\mu)\left[\frac{\partial S_{\mathbf{K}}^{(1)}}{\partial\mu}\right]-\left[\frac{\partial S_{\mathbf{K}}^{(0)}}{\partial\mathbf{R}}\right]\cdot\nabla\zeta\right]^2-\left[\left[\frac{\partial S_{\mathbf{K}}^{(0)}}{\partial\mathbf{R}}\right]\cdot\nabla\zeta\right]^2=2M_G[E-V(\mu)]-\left[\frac{\partial S_{\mathbf{K}}^{(0)}}{\partial\mathbf{R}}\right]^2, \tag{25}$$

so that by neglecting the second-order term on the left-hand side of this equation we obtain

$$(\chi\mu)\left[\frac{\partial S_{\mathbf{K}}^{(1)}}{\partial\mu}\right]=\hbar\mathbf{K}\cdot\nabla\zeta\pm\hbar[k_z^2-2M_GV(\mu)/\hbar^2]^{1/2}\ , \tag{26}$$

which can be easily integrated to yield

$$S_{\mathbf{K}}^{(1)}(\mathbf{R},\mu)=\hbar\mathbf{K}\cdot\mathbf{R}+\left[\frac{1}{\chi}\ln\mu\right]\hbar\mathbf{K}\cdot\nabla\zeta\pm\widetilde{S}(\mu)\ . \tag{27}$$

The solution of Eq. (21) to higher orders is considerably more complicated due to the appearance of terms including second derivatives of $\zeta(\mathbf{R})$. For example, to obtain $S_{\mathbf{K}}$ to second order in $\nabla\zeta$ we substitute the first-order expression for $\partial S_{\mathbf{K}}/\partial\mathbf{R}$ [i.e., $\hbar\mathbf{K}+(1/\chi)(\ln\mu)\hbar\mathbf{K}\cdot\nabla\nabla\zeta$] into Eq. (21) and neglect all terms which are of order higher than $(\nabla\zeta)^2$. Note that $\nabla\nabla\zeta$ is considered here of the same order as $\nabla\zeta$ (see below). Under these circumstances one gets the equation

$$\begin{aligned}(\chi\mu)[1+(\nabla\zeta)^2]^{1/2}\left[\frac{\partial S_{\mathbf{K}}^{(2)}}{\partial\mu}\right]&=\hbar k_z(\nabla\zeta\cdot(\mathbf{K}/k_z)+\ln\mu[\nabla\zeta\cdot(\nabla\nabla\zeta/\chi)\cdot(\mathbf{K}/k_z)]\\&\quad\pm\{W^2(\mu)-2\ln\mu[(\mathbf{K}/k_z)\cdot(\nabla\nabla\zeta/\chi)\cdot(\mathbf{K}/k_z)]\\&\quad+[\nabla\zeta\cdot(\mathbf{K}/k_z)]^2-(\ln\mu)^2[(\mathbf{K}/k_z)\cdot\nabla\nabla\zeta/\chi]^2\}^{1/2})\ .\end{aligned} \tag{28}$$

Note that Eq. (28) has the correct time-reversal symmetry since all the terms on the right-hand side of Eq. (28) outside the square root are odd functions of $\mathbf{K}$ so that they change sign by transforming $\mathbf{K}$ to $-\mathbf{K}$, while all the terms inside the square root are even functions of $\mathbf{K}$, a property which ensures that under time-reversal transformation (i.e., $\mathbf{K}\rightarrow-\mathbf{K}$ and incident wave$\rightarrow$reflected wave) the action $S_{\mathbf{K}}$ changes sign (time-reversal symmetry). The iterative procedure described above does not yield a systematic expansion of $S_{\mathbf{K}}$ in terms of a small parameter associated with the corrugation. Equation (28), for example, includes, in addition to the linear and quadratic terms in $\nabla\zeta$, a linear term (and higher-order terms) in $\nabla\nabla\zeta/\chi$. To compare the relative magnitudes of the various terms appearing in Eq. (28), we consider a 1D harmonic corrugation function of the form $\zeta(x)=h\cos(2\pi x/a)$, where h is the corrugation amplitude and a is the size of the surface unit cell.

A convergence criterion for the expansion appearing in Eq. (28) can be expressed in terms of the parameter

$$\epsilon\equiv\max\left|\frac{d\zeta(x)}{dx}\right|=\frac{2\pi h}{a}\ . \tag{29}$$

The structure of Eq. (28) clearly indicates, however, that such a criterion (e.g., $\epsilon\ll1$) would not be sufficient in general. All the derivatives of $\zeta(x)$ with respect to x, which should appear in the expansion to higher orders in the iteration process, are of first order in ϵ. For example, the dominant term of this type [appearing in Eq. (28)] can be represented by the parameter

$$\max\left|\left[\frac{d^2\zeta(x)}{dx^2}\right]\Big/\chi\right| = \frac{2\pi}{\chi a}\epsilon\ , \tag{30}$$

which is linear in ϵ. Higher-order terms of this type, which should be represented by the parameters

$$\max\left|\left[\frac{d^n\zeta(x)}{dx^n}\right]\Big/\chi^n\right| = \left[\frac{2\pi}{\chi a}\right]^n\epsilon\ ,$$

are all linear in ϵ.

Thus, the convergence of our expansion would depend not only on the smallness of ϵ but also on the smallness of another parameter $(2\pi/\chi a)$. The latter is small if χ is sufficiently large (i.e. if the potential is hard on the length scale a) such that

$$\chi a \gg 2\pi\ . \tag{31}$$

Unfortunately this is not the situation in a typical scattering experiment.

Considering Eq. (28) more closely, however, it is seen to be the beginning of a systematic expansion in the parameter $(\mathbf{K}/k_z)$. The magnitude of this parameter for the most important values of $\mathbf{K}$ in the scattering from $\mathbf{p}$ to $\mathbf{p}'$ can be estimated from the SP condition discussed in detail in Sec. II. In Appendix A we show that the most important value of $\mathbf{K}$ is related to the value of $\nabla\zeta$ at the stationary point via

$$\left[\mathbf{K}-\frac{1}{\hbar}\mathbf{P}\right] = \frac{1}{\hbar}p_z\nabla\zeta(\mathbf{R}_0)\ , \tag{32}$$

where $\mathbf{R}_0$ stands for the lateral coordinates of the stationary point. Thus if we take $\mathbf{P}=0$ (i.e., normal-incident conditions), $\mathbf{K}=(1/\hbar)p_z\nabla\zeta$ and

$$\hbar k_z = (p^2-\hbar^2K^2)^{1/2} = p_z[1-(\nabla\zeta)^2]^{1/2} \approx p_z$$

so that

$$\mathbf{K}/k_z \approx \nabla\zeta(\mathbf{R}_0)\ . \tag{33}$$

Note that if the incident angle is finite but sufficiently small such that $|\mathbf{P}/p_z| \le |\nabla\zeta(\mathbf{R}_0)|$, Eq. (33) is still essentially correct.

The above analysis shows that under near-normal-incidence conditions, the important values of $\mathbf{K}/k_z$ are of the order of the small parameter ϵ, so that the whole expansion represented by Eq. (28) can be regarded as a systematic expansion in ϵ. In particular, all the terms in Eq. (28) which include second derivatives of $\zeta(\mathbf{R})$ are at least of the order ϵ^3.

It turns out that the actual convergence of this expansion at the stationary point is significantly faster. This is due to the fact that at the stationary point the terms in Eq. (28) which include $\nabla\nabla\zeta$ cancel each other to fourth order in ϵ (see Appendix B). In conclusion of this section it is found that Eq. (28) provides a systematic expansion of the action $S_{\mathbf{K}}$, which converges quite rapidly at the stationary point under near-normal-incidence conditions.

IV. A SIMPLE KIRCHOFF-LIKE EXPRESSION FOR THE T MATRIX

In this section we shall derive an approximate analytic expression for the T matrix, assuming weak corrugation and near-normal-incidence conditions. These assumptions will allow us to use a simplified version of Eq. (28), which can be easily integrated analytically, and then, by plugging the resulting expressions for $S_{\mathbf{K}}^{\mathrm{inc,ref}}$ into Eq. (10), to derive a very simple expression for the T matrix. Physically the assumptions mentioned above amount to minimizing multiple-scattering effects. Within the HCW model, for which there is a complete localization of the sources generating the scattered waves in a two-dimensional surface, these assumptions lead to the well-known Kirchoff formula.[11,12]

In the light of our discovery (Sec. II) that soft potentials tend also to localize the scattering sources, it is therefore expected that a Kirchoff-like formula can be derived in this case under the above simplifying assumptions.

Following the discussion of Sec. III we neglect all the terms in Eq. (28) which include $\nabla\nabla\zeta$. We then expand the square roots to second order in $\nabla\zeta$ and integrate the equation over μ. The result can be written as

$$\frac{1}{\hbar}S_{\mathbf{K}}^{\mathrm{inc,ref}}(\mathbf{R},\mu) = \mathbf{K}\cdot\mathbf{R} + \frac{1}{\chi}\ln\mu(\mathbf{K}\cdot\nabla\zeta) \pm \left[[-\tfrac{1}{2}(\nabla\zeta)^2]\frac{1}{\hbar}\tilde{S}(\mu) + \frac{1}{2\chi k_z}\ln\left[\frac{2\mu}{1+W(\mu)+\gamma\mu}\right](\mathbf{K}\cdot\nabla\zeta)^2\right]\ . \tag{34}$$

We know from Sec. II that the dominant contributions to the scattering amplitude come from values of μ near $\mu=2$ (i.e., $V=0$), where $W(\mu)=1$ [see Eq. (24)]. Since we assume that $\gamma \ll 1$ (i.e., E_i much larger than D), $1+W(\mu)+\gamma\mu \simeq 2$, and we may replace the logarithm in the last term on the right-hand side of Eqs. (34) by $\ln\mu$. Using the resulting expressions for $S_{\mathbf{K}}^{\mathrm{inc,ref}}$ in Eqs. (9) and (10) we obtain

$$T(\mathbf{p},\mathbf{p}') \approx (\overline{|p_z|}/|p_zp_z'|)\left[\frac{M_GD}{\hbar\chi}\right]^2\int_0^\infty d\mu_1(\mu_1-2)/[W(\mu_1)]^{1/2}\int_0^\infty d\mu_2(\mu_2-2)Q_{\mathbf{p},\mathbf{p}'}(\mu_1\mu_2)/[W(\mu_2)]^{1/2}\ , \tag{35}$$

where

$$Q_{\mathbf{p},\mathbf{p}'}(\mu_1,\mu_2)\equiv\frac{1}{4\pi^2\Omega}\int\frac{d^2K}{\hbar k_z}\int d^2R_1\int d^2R_2\exp\left[\frac{i}{\hbar}[\mathbf{P}\cdot\mathbf{R}_1-\mathbf{P}'\cdot\mathbf{R}_2+p_z\zeta(\mathbf{R}_1)-p_z'\zeta(\mathbf{R}_2)]\right]$$
$$\times\exp\{i[\mathbf{K}\cdot(\mathbf{R}_2-\mathbf{R}_1)+(k_z/X)(U_{p_z}(\mathbf{K},\mathbf{R}_1)\ln\mu_1-U_{p_z'}(\mathbf{K},\mathbf{R}_2)\ln\mu_2$$
$$-\{1-\tfrac{1}{2}[\nabla\hbar(R_1)]^2\}\Phi(\mu_1)$$
$$-\{1-\tfrac{1}{2}[\nabla\hbar(\mathbf{R}_2)]^2\}\Phi(\mu_2))]\}\ , \tag{36}$$

$$U_{p_z}(\mathbf{K},\mathbf{R}_1)\equiv\left[\frac{1}{\hbar}p_z-\mathbf{K}\cdot\nabla\zeta(\mathbf{R}_1)-[\mathbf{K}\cdot\nabla\zeta(\mathbf{R}_1)]^2/2k_z\right]\Big/k_z\ , \tag{37}$$

$$U'_{p_z}(\mathbf{K},\mathbf{R}_2)\equiv\left[\frac{1}{\hbar}p_z'-\mathbf{K}\cdot\nabla\zeta(\mathbf{R}_2)+[\mathbf{K}\cdot\nabla\zeta(\mathbf{R}_2)]^2/2k_z\right]\Big/k_z\ , \tag{37'}$$

and

$$\Phi(\mu)\equiv W(\mu)+\ln\{2\mu/[1+\gamma\mu+W(\mu)]\}-\sqrt{\gamma}\sin^{-1}[\sqrt{\gamma}(1-\mu)/\sqrt{1+\gamma}]=\frac{1}{\hbar}(X/k_z)\tilde{S}(\mu)\ . \tag{38}$$

Transforming the integration variables $\mathbf{R}_1,\mathbf{R}_2$ to

$$\mathbf{R}\equiv\tfrac{1}{2}(\mathbf{R}_1+\mathbf{R}_2),\ \ \boldsymbol{\rho}\equiv\mathbf{R}_1-\mathbf{R}_2 \tag{39}$$

we expand $\zeta(\mathbf{R}_1),\zeta(\mathbf{R}_2)$ and $\nabla\zeta(\mathbf{R}_1),\nabla\zeta(\mathbf{R}_2)$ about the mean position $\mathbf{R}$ in every place they appear in Eqs. (36) and (37). The expansion parameter $\boldsymbol{\rho}$ is essentially the lateral distance traveled by the particle within the scattering region. Under the simplifying conditions assumed above (i.e., weak corrugation and normal incidence) the important values of $|\boldsymbol{\rho}|$ should be much smaller than the size of the surface unit cell a (see later for a justification of this point). We may therefore linearize the expansion, a procedure which is consistent with our use of the truncated expansion of $S_{\mathbf{K}}$ in derivatives of $\zeta(\mathbf{R})$. Performing the integrations over $\boldsymbol{\rho}$ and over $\mathbf{K}$ in Eq. (36) by the SP method, Eq. (35) is reduced to

$$T(\mathbf{p},\mathbf{p}')\approx\overline{|p_z|}/|p_zp_z'|$$
$$\times\Omega^{-1}\int d^2R\,BB'\hbar k_{z,0}\exp\left[\frac{i}{\hbar}[(\mathbf{P}-\mathbf{P}')\cdot\mathbf{R}+(p_z-p_z')\zeta(\mathbf{R})]\right]\ , \tag{40}$$

where

$$B\equiv2(k_{z,0}\gamma/iX)\int_0^\infty d\mu(\mu-2)\times\exp[i(k_{z,0}/X)f(\mu)]/\sqrt{W(\mu)}\ , \tag{41}$$

$$f(\mu)\equiv U\ln\mu-\{1-\tfrac{1}{2}[\nabla\zeta(\mathbf{R})]^2\}\Phi(\mu)\ . \tag{42}$$

U and U' are shortened notations for $U_{p_z}(\mathbf{K}_0,\mathbf{R})$ and $U'_{p_z}(\mathbf{K}_0,\mathbf{R})$, respectively, and B' is obtained from Eq. (41) by replacing U with $-U'$ in Eq. (42). The stationary point $\mathbf{K}_0$ for the integration over $\mathbf{K}$ is approximately given by $\hbar\mathbf{K}_0\approx\frac{1}{2}(\mathbf{P}+\mathbf{P}')$, and $\hbar k_{z,0}=(p^2-\hbar^2K_0^2)^{1/2}$, while the stationary point $\boldsymbol{\rho}_0$ for the integration over $\boldsymbol{\rho}$ is roughly $\boldsymbol{\rho}_0\sim(\mathbf{K}_0/k_{z,0})/X$. For near-normal incidence this means that $|\boldsymbol{\rho}_0|/a\sim|\nabla\zeta|/aX\leq\epsilon/(aX)\ll1$, justifying our linearization assumption made previously in this section.

The classical limit of the T matrix, given by Eq. (40), is obtained when the integrals over μ [Eq. (41)] and over $\mathbf{R}$ [Eq. (40)] are performed by the SP method. The SP equation for the former integral is

$$W(\mu)=U/[1-\tfrac{1}{2}(\nabla\zeta)^2]\equiv\tilde{U}\ , \tag{43}$$

yielding for the stationary point μ_0

$$\mu_0=1+[1+(1-\tilde{U}^2)/\gamma]^{1/2}\ . \tag{44}$$

Expanding $f(\mu)$ about μ_0 to second order and replacing $\sqrt{W(\mu)}$ in the denominator of the integrand in Eq. (41) by its value at the stationary point μ_0 we obtain

$$B=-[2\lambda i/(\tilde{U})^{1/2}]\int_0^\infty d\mu(\mu-2)e^{i\lambda\alpha(\mu-\mu_0)^2}\times e^{i(k_{z,0}/X)f(\mu_0)}\ , \tag{45}$$

where

$$\lambda\equiv k_{z,0}\gamma/4X \tag{46a}$$

and

$$\alpha\equiv2(\mu_0-1)/\mu_0\tilde{U}\ . \tag{46b}$$

The SP equation for the integral over $\mathbf{R}$ is, to first order in ϵ, given by

$$(\mathbf{P}-\mathbf{P}')+(p_z-p_z')\nabla\zeta(\mathbf{R})=0\ . \tag{47}$$

Using this equation we obtain that, to second order in ϵ, $\widetilde{U}=-\widetilde{U}'=1$, $\mu_0=\mu_0'=2$, and $\alpha=\alpha'=1$. For these values of the parameters the integral in Eq. (45) can be readily calculated with the results

$$B=B'=\exp\{i[(k_{z,0}/\chi)f(2)+4\lambda]\}\ , \qquad (41')$$

so that the T matrix in the classical limit takes the simple Kirchoff-like form[11,12]

$$T_{\text{classical}}(\mathbf{p},\mathbf{p}')=\overline{(|p_z|}^2/|p_zp_z'|)\frac{1}{\Omega}\int_{\text{SP}}d^2R\,\exp\left[\frac{i}{\hbar}[(\mathbf{P}-\mathbf{P}')\cdot\mathbf{R}+(p_z-p_z')\zeta(\mathbf{R})]\right]. \qquad (48)$$

Note that for a flat potential [i.e., $\nabla\zeta(\mathbf{R})=0$] Eq. (45) for B coincides with Eq. (15) for the reflection amplitude $f(p_z;0)$ in one dimension. As already mentioned in Sec. II, we have tested the validity of the approximation made in deriving Eq. (45) from the exact formula for B [Eq. (41)] by comparing the result of an exact numerical integration applied to Eq. (41) with the result of integrating a modified version of Eq. (41), in which $W(\mu)$ is replaced by unity [see Fig. (1)]. Despite the large difference between the two integrands near the classical turning point [where $W(\mu)=0$], the results of the integrations are very close, both yielding almost unity for the reflection coefficient.

Furthermore, we have also tested the validity of the SP procedure applied to Eq. (41) in the classical limit [see Eq. (45) with $\mu_0=2$, $\alpha=1$] by comparing the result [Eq. (41′)] to that obtained by applying exact numerical integration to Eq. (41). For $k_{z,0}a=107.35$, $\chi a=3.124$, $\gamma=0.0102$, so that $\lambda=0.0878$, Eq. (41′) yields

$$\text{Re}B=-0.8548,\quad \text{Im}B=-0.519\ ,$$

while the exact numerical integration yields in this case

$$\text{Re}B=-0.855,\quad \text{Im}B=-0.517$$

in excellent agreement!

V. RESULTS AND DISCUSSION

The result of the classical approximation used in Sec. IV [Eq. (48)] shows that the scattering cross section from a weakly corrugated Morse potential, defined by Eq. (19), follows, on the average, the classical envelope of the corresponding diffraction pattern from a HCW for the same corrugation function, provided that the incident beam is perpendicular to the nominal surface plane.

It is therefore of interest to compare the results obtained from the two model potentials under similar conditions when quantum-mechanical (QM) effects are taken into account. In Fig. 2 we plot the results of diffraction intensities obtained by applying numerical integration to Eqs. (40) and (41); we use a 1D harmonic corrugation function $\zeta(x)=h\cos(2\pi x/a)$ and typical values for the parameters corresponding to He diffraction by Cu(110).[2] We also plot in this figure the results obtained from the corresponding HCW model in the Kirchoff approximation.

The accuracy of the method used is tested by checking two quantities: (1) The value of $|BB'|$ [Eq. (41)] for the specular peak at a point x where $d\zeta/dx=0$ (e.g., $x=0$), (2) The sum over all diffraction probabilities. Both (1) and (2) are known in general to be exactly equal to unity.

In Table I we present the results of such tests for $h/a=0.012$. As expected, the deviation of the numerically computed value of $|B(0)B'(0)|$ from unity is found to decrease systematically with increasing values of the incident wave number k_i. The unitarity test shows essentially the same behavior as a function of k_i.

The results exhibited in Fig. 2 clearly show that for a weak corrugation [Fig. 2(a)] the QM scattering probabilities for our soft potential are very close to the corresponding QM Kirchoff probabilities. In Fig. 2(b) we present similar results for a corrugation amplitude twice as large as in Fig. 2(a) (i.e., $h/a=0.024$). Our unitarity tests for this relatively large corrugation yield quite reasonable re-

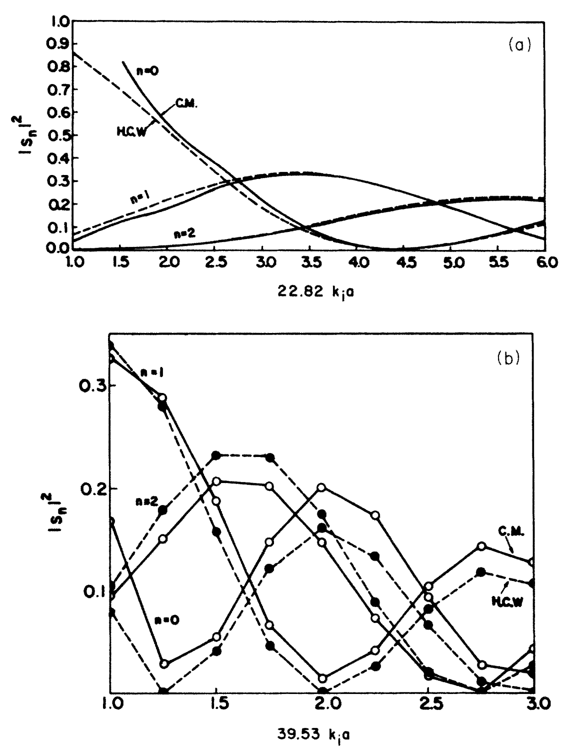

FIG. 2. Diffraction probabilities $|S_n|^2$, obtained by integrating numerically Eqs. (40) and (41) [solid lines in (a) and empty circles in (b)] and as obtained from the Kirchoff formula, i.e., from Eq. (40) with $B(\mathbf{R})B'(\mathbf{R})=1$ [dashed lines in (a) and solid circles in (b)], for the specular peak ($n=0$) and the first two diffraction peaks ($n=1,2$), as functions of the wave number k_i of the incident beam. The angle of incidence is $\theta_i=0$. A 1D harmonic corrugation function $\zeta(x)=h\cos(2\pi x/a)$ is used with $h/a=0.012$ in (a) and $h/a=0.024$ in (b). The other potential parameters used are $\chi a=3.78$ and $D=6.3$ meV. The value of the incident energy E_i corresponding to $k_ia=39.53$ is $E_i=63$ meV.

TABLE I. Accuracy tests for the Kirchoff-like formula [Eq. (40)]; values of $|B(0)B'(0)|$ for the specular channel are presented in the second column. The corresponding unitarity tests are given in the third column. For comparison, we give in the fourth column the corresponding unitarity tests for the Kirchoff formula [Eq. (40)] with $B(x)B'(x)=1$. The potential parameters used in these tests are $\chi a=3.78$, $D=6.3$ meV, and $h/a=0.012$. ($E_i=21$ meV for $k_i a=22.82$.)

$k_i a$	$\lvert B(0)B'(0)\rvert$ (Specular)	Unitarity CM	Unitarity HCW
22.82	0.9105	0.864	0.997
34.23	1.0278	1.087	0.997
45.64	0.9539	0.928	0.997
57.06	0.9927	0.998	0.997
68.47	0.9931	0.997	0.997
79.88	0.9909	0.990	0.997
91.29	0.9955	0.998	0.997
102.70	0.9960	0.998	0.997
114.11	0.9965	0.999	0.997
125.52	0.9974	1.001	0.997
156.94	0.9977	1.001	0.997

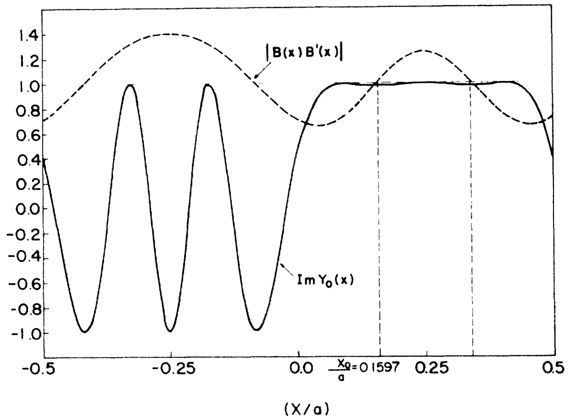

FIG. 3. The imaginary part of the exponential

$$Y_0(x)\equiv\exp\left[\frac{i}{\hbar}[(p_x-p_x')x+(p_z-p_z')\zeta(x)]\right],\quad p_x=0$$

(solid line) and the absolute value of the preexponential factor $B(x)B'(x)$ (dashed line), as functions of x within the surface unit cell $-a/2<x\leq a/2$, for the third diffraction channel. A 1D harmonic corrugation function is used with $h/a=0.0132$. The other parameters used are $k_i a=135.36$, $\chi a=3.015$, and $\gamma_0\equiv D/E_i=0.067\,75$.

sults (5% deviation in the worst case). The differences between the diffraction probabilities obtained for our soft potential and those obtained from the Kirchoff formula are significantly larger than before. Yet these differences remain small compared to the probabilities themselves so that one can conclude that even for such a larger corrugation amplitude the HCW model is still a good approximation. The reason for this rather surprising agreement between the two model potentials may be illuminated by considering the integrand in Eq. (40). In Fig. 3 we plot the amplitude $B(x)B'(x)$ and the exponential

$$\exp\left[\frac{i}{\hbar}(p_x-p_x')x+(p_z-p_z')\zeta(x)\right]$$

in a typical case. We select a sufficiently larger value for the incident wave number k_i such that the exponential completes several oscillations within the surface unit cell. The Kirchoff result is obtained if $B(x)B'(x)=1$ everywhere. For our soft potential the amplitude $B(x)B'(x)$ is not constant; its variation increases with increasing k_i or with the corrugation amplitude.

As can be clearly seen in Fig. 3, $|B(x)B'(x)|$ oscillates almost symmetrically about its value at the stationary point x_0. The latter value is found in our exact numerical calculation to be equal to unity, in agreement with the classical result [Eq. (41')]. Thus the integral over x in Eq. (40) is not significantly different from the corresponding integral in the Kirchoff formula due to cancellation of contributions originating to the left and to the right of the stationary point x_0.

The remarkable similarity between the scattering from our CM potential and the scattering by a HCW, found here, may be indicative of the existence of universality not only in reflection from 1D potentials but also in scattering by three-dimensional (3D), weakly corrugated potentials under normal incidence conditions. Some supportive evidence for this conjecture is very encouraging.[22] For example, numerical computations of diffraction probabilities for a somewhat different version of the CM potential; that is, a Morse potential corrugated only in the repulsive part,

$$V(\mathbf{R},z)=De^{2\chi[z-\phi(\mathbf{R})]}-2De^{\chi z}\,, \tag{49}$$

have been reported by several authors.[15,26–28] In Table II we present the results of such an exact numerical computation[28] as applied to a model of Ne/W(110). In the weak corrugation limit Eq. (49) coincides with the model potential used in Ref. 28.

This model potential provides an interesting test for our conjecture. For potential energies between zero and D, the shape of the equipotential surfaces is a strong function of energy.[29] Only for sufficiently high values of V, such that $V\gg D$, does the corrugation $\zeta(\mathbf{R})$ of the equipotential surfaces become identical to the corrugation function $\phi(\mathbf{R})$ of the repulsive part of the potential. At vanishing potential, $\zeta(\mathbf{R})=2\phi(\mathbf{R})+\text{const}$. For the case considered in Table II, the corrugation $\zeta(\mathbf{R})$ of the classical turning surface ($V=E_i=63$ meV) is given by $\zeta(\mathbf{R})\approx1.21\phi(\mathbf{R})+\text{const}$.

In the light of the large difference between the two corrugation functions it is very interesting to compare the results of computations based on the Kirchoff formula for each of the corrugation functions mentioned above with the result of the exact numerical calculation. The outcome of such a comparison is remarkable: While the use of the corrugation function at the classical turning surface yields very poor agreement with the exact diffraction probabilities, our vanishing potential criterion for the corrugation function yields diffraction probabilities which agree *quantitatively* with the exact ones. Additional evidence which supports our conjecture can be found in Refs.

TABLE II. Comparison between diffraction probabilities obtained by solving exactly close coupling equations for the CM potential given by Eq. (49) (Ref. 28) and the corresponding diffraction probabilities obtained from the Kirchoff formula. A harmonic corrugation function $\phi(x,y)=h\cos(2\pi x/a)+h\cos(2\pi y/a)$ is used in the Morse potential with $h/a=0.0033$. Two sets of data are presented for the HCW model. The first corresponds to a corrugation function $\zeta(\mathbf{R})=2\phi(\mathbf{R})$ (the corrugation at vanishing potential), while the second corresponds to $\zeta(\mathbf{R})=1.2\phi(\mathbf{R})$ (the corrugation at the classical turning surface). The other parameters used are $\chi a=3.015$, $k_i a=67.68$, $\gamma_0\equiv D/E_i=0.271$, and $\theta_i=0$.

Peak (nm)	Exact	HCW $\zeta(\mathbf{R})=2\phi(\mathbf{R})$	HCW $\zeta(\mathbf{R})=1.2\phi(\mathbf{R})$
00	0.4016	0.4309	0.741 77
10	0.1099	0.1068	0.0585
20	0.0061	0.0056	0.0011
30	0.000 14	0.000 12	$<10^{-5}$
11	0.0299	0.0265	
22	0.0001	0.000 07	
21	0.0017	0.001 38	

22 and 6.

Finally, we would like to point out that the importance of the potential corrugation near vanishing potential, as emerges from our work, seems to be in accord with the recent surprising observation of pronounced neon diffraction from Ni(110) and Pd(110),[30] which indicates that the corrugation amplitudes are much larger for Ne than for He! We believe that such an effect may be due to the fact that the well depth for Ne/Ni(110) is considerably (about twice) larger than the well depth for the He/Ni(110).[29] Such a large increase in the potential well should have a big effect on the location (and shape) of the vanishing potential surface, much more significant than on the classical turning surface.

As pointed out recently by Liebsch and Harris,[31] a larger well depth D may cause the physisorption minimum and therefore the classical turning points to lie closer to the surface-ion cores, so that a slightly stronger corrugation is expected if the corrugation function is defined at the classical turning surface. The dramatic increase in the corrugation reported experimentally indicates, however, that the definition proposed in the present paper for the corrugation function (i.e., at $V=0$) is more appropriate.

APPENDIX A

In this appendix we derive the relation (32). To do so we shall use the first-order approximation for $S_{\mathbf{K}}^{\text{inc}}$ [Eq. (27)] in Eq. (10). The corresponding expression for $f(\mathbf{p},\mathbf{K})$ can be written in the form

$$f(\mathbf{p};\mathbf{K})=(M_G D/i\hbar p_z\chi)\int d^2R\,\exp\left\{\left[\left[\frac{1}{\hbar}\mathbf{P}-\mathbf{K}\right]\cdot\mathbf{R}+\frac{1}{\hbar}p_z\zeta(\mathbf{R})\right]\right\}$$

$$\times\int_0^\infty d\mu(\mu-2)\exp\left[i\left[(k_z/\chi)U\ln\mu-\frac{1}{\hbar}\tilde{S}(\mu)\right]\right]\Big/\sqrt{W(\mu)}\;, \qquad \text{(A1)}$$

with

$$U\equiv\left[\frac{1}{\hbar}p_z-\mathbf{K}\cdot\nabla\zeta(\mathbf{R})\right]\Big/k_z\;. \qquad \text{(A2)}$$

The stationary point for the integral over μ is determined from

$$W(\mu_0)=U\;, \qquad \text{(A3)}$$

while the SP equation for the integral over $\mathbf{R}$ is

$$\left[\frac{1}{\hbar}\mathbf{P}-\mathbf{K}\right]+\frac{1}{\hbar}p_z\cdot\nabla\zeta(\mathbf{R})-k_z(\mathbf{K}/k_z)\cdot[\nabla\nabla\zeta(\mathbf{R})/\chi]\ln\mu=0\;. \qquad \text{(A4)}$$

The last term on the right-hand side of Eq. (A4) is of second order. The neglect of this term yields the desired equation, (32).

APPENDIX B

In this appendix we show that under normal-incidence conditions the linear terms in $\nabla\nabla\zeta$ in Eq. (28) cancel each other to fourth order in ϵ. To show this let us neglect the last two terms within the square root in Eq. (28) since they are of the order ϵ^4. We then expand, to lowest order, the square root about $W(\mu)$. The result is

$$(\chi\mu)[1+\tfrac{1}{2}(\nabla\zeta)^2]\left[\frac{\partial S_{\mathbf{K}}^{(2)}}{\partial\mu}\right]=\hbar k_z\{\nabla\zeta\cdot(\mathbf{K}/k_z)+W(\mu)+\ln\mu(\mathbf{K}/k_z)\cdot(\nabla\nabla\zeta/\chi)\cdot[\nabla\zeta-(\mathbf{K}/k_z)/W(\mu)]\}\;. \qquad \text{(B1)}$$

Now at the stationary point μ_0 [see Eq. (A3)], $W(\mu_0)=U$, while at $\mathbf{R}_0$, $\nabla\zeta(\mathbf{R}_0)=\mathbf{K}/k_z$ [Eq. (33)]. Therefore, by Eq. (A2) one has

$$U(\mathbf{R}_0)=\left[\frac{1}{\hbar}p_z-k_z(\nabla\zeta)^2\right]\Big/k_z=1+O(\nabla\zeta)^2\ ,$$

so that at the stationary point $(\mathbf{R}_0,\mu_0)$

$$\nabla\zeta(\mathbf{R}_0)-(\mathbf{K}/k_z)/W(\mu_0)\approx\nabla\zeta(\mathbf{R}_0)[1-1/U(\mathbf{R}_0)]$$
$$=O(\nabla\zeta(\nabla\zeta)^2)\ . \qquad \text{(B2)}$$

Thus under normal-incidence conditions the last term on the right-hand side of Eq. (B1) is of the order of ϵ^5.

[1]G. Drolshagen and E. J. Heller, J. Chem. Phys. **79**, 2072 (1983).

[2]J. Perreu and J. Lapujoulade, Surf. Sci. **119**, 1292 (1982); G. Armand, J. Lapujoulade, J. R. Manson, J. Perreu, and B. Salamon, Israel J. Chem. **22**, 298 (1982).

[3]G. Armand and J. R. Manson, Phys. Rev. Lett. **43**, 1839 (1979).

[4]G. Armand, J. Phys. (Paris) **41**, 1475 (1980).

[5]G. Armand and J. R. Manson, Surf. Sci. **119**, L299 (1982).

[6]G. Drolshagen, A. Kaufhold, and J. P. Toennies, Israel J. Chem. **22**, 283 (1982).

[7]R. B. Gerber, A. T. Yinon, Y. Shimoni, and D. J. Kouri, J. Chem. Phys. **73**, 4397 (1980).

[8]R. Shinke, J. Chem. Phys. **76**, 2352 (1982).

[9]J. M. Bowman and S. C. Park, J. Chem. Phys. **76**, 1168; **77**, 5441 (1982).

[10]J. C. Polanyi and J. P. Wolf, Ber. Bunsenges. Phys. Chem. **86**, 356 (1982).

[11]U. Garibaldi, A. C. Levi, R. Spandacini, and G. E. Tommei, Surf. Sci. **48**, 649 (1975).

[12]M. V. Berry, J. Phys. A **8**, 566 (1975).

[13]T. Engel and K. H. Rieder, *Structural Studies of Surfaces* (Springer-Verlag, Berlin, 1982).

[14]R. B. Laughlin, Phys. Rev. B **25**, 2222 (1982).

[15]M. J. Cardillo, G. E. Becker, D. R. Hamann, J. A. Serri, L. Whitman, and L. F. Mattheiss, Phys. Rev. B **28**, 494 (1979).

[16]G. Benedek, G. Brusdeylins, L. Miglio, R. Rechsteiner, J. G. Skofronick, and J. P. Toennies (unpublished).

[17]G. Brusdeylins and J. P. Toennies, Surf. Sci. **126**, 647 (1983).

[18]H. D. Meyer, Surf. Sci. **104**, 117 (1981).

[19]G. Doyen and T. B. Grimley, Surf. Sci. **91**, 51 (1980).

[20]D. Evans, V. Celli, G. Benedek, J. P. Toennies, and R. B. Doak, Phys. Rev. Lett. **50**, 1854 (1983).

[21]D. Reidel, D. Eichenauer, and J. P. Toennies, in *Proceedings of the 17th Jerusalem Symposium on the Dynamics of Molecule-Surface Interactions,* edited by B. Pullman and J. Jortner (Reidel, Dordrecht, 1984).

[22]T. Maniv and M. H. Cohen, Phys. Rev. Lett. **53**, 78 (1984).

[23]T. Maniv and M. H. Cohen, Phys. Rev. B **19**, 4883 (1979).

[24]P. A. Dirac, *The Principles of Quantum Mechanics* (Clarendon, Oxford, 1947).

[25]W. H. Miller, Adv. Chem. Phys. **25**, 69 (1974).

[26]R. B. Gerber and A. T. Yinon, J. Chem. Phys. **73**, 3232 (1980).

[27]G. Wolken, Jr., J. Chem. Phys. **58**, 3047 (1973).

[28]H. Chow, Surf. Sci. **62**, 487 (1977); **66**, 221 (1977).

[29]H. Hoinkes, Rev. Mod. Phys. **52**, 933 (1980).

[30]K. H. Rieder and W. Stocker, Phys. Rev. Lett. **52**, 352 (1984).

[31]A. Liebsch and J. Harris, Surf. Sci. **130**, L349 (1983).